Astron. Astrophys. 362, 1008–1019 (2000)

ASTRONOMY AND ASTROPHYSICS

Evolutionary status of hydrogen-deficient central stars of planetary nebulae

S.K. Górny and R. Tylenda

Copernicus Astronomical Center, Department for Astrophysics, Rabiańska 8, 87-100 Toruń, Poland

Received 13 June 2000 / Accepted 4 September 2000

Abstract. The observational data for the planetary nebulae with hydrogen-deficient central stars are analysed. We show that the general evolutionary sequence is: late-[WC], early-[WC], PG 1159. An analysis of the observed distributions of nebular parameters leads to a conclusion that the planetary nebulae with hydrogen-deficient nuclei are not different from the population of other planetary nebulae in the Galaxy. In particular the proportion of the H-deficient stars among young nebulae is the same as in the whole population. We have made a detailed comparison of the observed parameters with theoretical modelling of the late He-shell flash (born again AGB) scenario. Our finding is that the [WC] nuclei are not formed in a late He-shell flash. This scenario can, however, give origin to some PG 1159 objects. There are five objects known which have presumably suffered from a late He-shell flash. The observed parameters of their nebulae imply that these stars will not become typical [WC] objects. Thus most of hydrogen-deficient central stars (at least [WC]) evolve directly from the AGB as do the other planetary nebula nuclei. We discuss implications of this result.

Key words: ISM: planetary nebulae: general – stars: AGB and post-AGB – stars: Wolf-Rayet

1. Introduction

In the observed population of planetary nebula nuclei (PNNi) several spectral classes can be distinguished, e.g. O, Of, sdO, WR, WR-Of (e.g. Lutz 1978). From the point of view of the evolutionary status of these stars the most important classification is, however, that deduced from analyses of their surface abundances. In this case the PNN population can be divided into two well defined groups, i.e. hydrogen-rich and hydrogen-deficient (Méndez 1991). In the first group hydrogen is a dominant element in the PNN atmosphere and its abundance is close to the cosmic value. In the second case the star atmosphere is practically hydrogen-free while helium and carbon are the most abundant elements.

From spectral appearances one can distinguish two classes of the H-deficient PNNi. The spectra of many H-deficient PNNi are dominated by strong and wide emission lines characteristic for the Wolf-Rayet stars. At present we know about 50 objects of this kind and all of them are of [WC] type. On the other side of this scheme we have PNNi whose spectra show predominantly absorption lines. Many stars from these group have been found to pulsate like PG 1159-035. A few H-deficient PNNi do not fit this simple scheme. For example, the central stars of the planetary nebulae A 30 and A 78 show absorption lines and weak emissions (WR-Of(C) type according to Méndez (1991). Another case is the central star of the nebula Longmore 4 which has been observed to change its spectral appearance from PG 1159 to [WC 2–3] and back (Werner et al. 1992). The WR-type emission lines are interpreted as evidence of stellar winds. Detailed analyses of spectra of the [WC] PNNi give mass loss rates typically of $10^{-6}\mathrm{M}_{\odot}$ yr^{-1}. No other type of PNNi has been observed to lose matter at such a high rate. Recent reviews on the H-deficient PNNi can be found in Hamann (1996, 1997), Napiwotzki et al. (1996), Tylenda (1996), Werner et al. (1996), and Lundström & Stenholm (1996).

It is not clear at present which evolutionary path gives origin to the H-deficient PNNi. The principal problem are the observed surface abundances. It is evident that the [WC] PNNi burn helium in a shell (e.g. Tylenda & Górny 1993). Some [WC] PNNi are surrounded by rather young and dense nebulae which suggests that these objects have recently left the asymptotic giant branch (AGB) after having formed the planetary nebula (PN) presumably during a helium-shell flash (e.g. Méndez 1991). Then it seems natural to suppose that the PG 1159 stars descend from the [WC] PNNi. This idea is supported by the fact that the surface abundances are similar in both types of stars and that the PG 1159 stars, contrary to the [WC] PNNi, have old, faint or no detectable PN.

There is a number of theoretical evolutionary tracks which produce He-burning PNNi after having left the AGB during a He-shell flash (Iben 1984; Wood & Faulkner 1986; Vassiliadis & Wood 1994). However, these model PNNi keep a H-rich envelope throughout the PN phase so they cannot be interpreted as model [WC] PNNi. One can adopt that an intense mass loss continues after AGB until all the H-rich matter is lost. When it happens the surface layers are of almost pure helium and mass loss has to be continued in order to expose layers where carbon is as abundant as helium. When this is achieved the He-rich envelope

Send offprint requests to: S.K. Górny (skg@ncac.torun.pl)

is, however, too small to maintain He-burning (Schönberner & Blöcker 1992). Thus a high luminosity necessary to power the WR-type wind is no longer ensured.

The observed surface abundances of the H-deficient PNNi can be much more easily explained in an evolutionary scenario of a very late He-shell flash (also called born again AGB). In this case a PNN which has already finished its high luminosity phase as a H-burner suffers from a He-shell flash in the cooling phase. The star quickly expands, goes back to the AGB and repeats the PNN evolution, this time as a He-burner. The rests of hydrogen are lost in a wind and/or mixed and burnt. Strong convective mixing dredges carbon up to the surface. For the first time the born again AGB scenario has been described and analysed by Iben at al. (1983) in their study of the PNe A 30 and A 78. More recently, this scenario has been applied to explain the observed abundances in the PG 1159 stars (Schönberner & Blöcker 1992; Iben & MacDonald 1995).

The third possibility has been invoked and discussed in Tylenda & Górny (1993) and involves the AGB evolution in binaries. Evolutionary calculations of AGB stars (e.g. Vassiliadis & Wood 1994) show that it is during He-shell flashes when the stellar radius achieves local maxima (at least for initial star masses below 3.5 $M_\odot$). Therefore one may argue that if an AGB star happens to fill its Roche lobe it takes place most probably during a He-shell flash. If the common envelope phase ends up with a complete loss of the H-rich envelope of the AGB star than the outcome would be a close binary with a luminous H-poor He-burning star. Unfortunately not a single [WC] or PG 1159 central star is known to be a binary so this idea does not seem to be the major evolutionary canal for the H-poor PNNi.

In this paper we make an extensive analysis of the observational data for PNe with H-deficient central stars. We concentrate on a discussion and interpretation of diagrams and plots involving basic observational data such as PNN magnitude, nebular Hβ flux and PN dimensions. First, we investigate the hypothesis that the [WC] subclasses of the WR-type PNNi and other H-deficient (mostly PG 1159 type) central stars form an evolutionary sequence. Next, we compare our sample of H-deficient PNNi and their nebulae with the rest of the Galactic PN population. Then, the observed distributions on diagrams are confronted with predictions of theoretical evolutionary considerations within the born again AGB scenario. Our conclusion is that the very late He-shell flash cannot be the major evolutionary path leading to the formation of the H-deficient PNNi, at least of those of the [WC] type. We also discuss observational data for a few cases of PNe whose nuclei have very probably undergone a late He-shell flash. We show that it is very unlikely that these objects could give birth of [WC] PNNi. Thus the direct evolution from the AGB, presumably triggered by the last AGB He-shell flash, seems to be the only reasonable scenario for origin of the majority of the H-deficient PNNi.

2. Observational data and parameters

Table 1 lists the PNe with H-deficient central stars and the observational data we have used in the present study. Column (1) lists the PN G numbers from the Strasbourg-ESO catalogue (Acker et al. 1992). Usual names of the objects are given in Column (2). Column (3) shows the spectral classes of the central stars. The angular diameters of the nebulae (in arcsec) can be found in Column (4). The nebular densities (in cm^{-3}) are given in Column (5). The observed Hβ fluxes (in erg $\mathrm{cm}^{-1}\,\mathrm{s}^{-1}$) and the radio fluxes at 6 cm (in mJy) are listed in Columns (6) and (7), respectively. Column (8) gives the Hα/Hβ line ratio. The central star B and V magnitudes are given in Columns (9) and (10), respectively.

The [WC] classification primarily comes from Tylenda et al. (1993) and Acker et al. (1999) with preferences given to the latter paper as it was based on a newer and better quality observational material. The classification of M 1-60 (019.7-04.5) is according to Acker et al. (1996) while that of NGC 2452 (243.3-01.0) and NGC 2867 (278.1-05.9) is from Koesterke & Hamann (1997).

Crowther et al. (1998) have recently classified [WC] PNNi with a somewhat different classification scheme as in the above studies. However, for the sake of uniformity of our data set we have decided not to use the results from this paper. They are given only for a limited sample (20 objects) and the classification criteria of Crowther at al. cannot be applied to other objects without having access to direct spectroscopic data.

For other H-deficient (non-[WC]) PNNi the classification comes from Dreizler et al. (1995) and Méndez (1991).

The angular diameters are primarily taken from the Strasbourg-ESO catalogue. In the case of small nebulae (angular diameter $< 10''$) we adopt preferentially the dimensions from VLA measurements. For He 2-113 (321.0+03.9) and He 2-1333 (332.9-09.9) the diameters are from de Marco et al. (1997).

The nebular densities, n_e, have been derived from the [S II] line ratio and come from Stanghellini & Kaler (1989), Acker et al. (1989, 1991), Kingsburgh & Barlow (1994), Cuisinier (1994), Philips (1998) and from other sources in individual cases.

The Hβ fluxes are from the Strasbourg-ESO catalogue. The radio fluxes are taken from the same compilation and references as in Stasińska et al. (1992). The values of the Hα/Hβ ratio come from Tylenda et al. (1994). The central star magnitudes are from the Strasbourg-ESO catalogue with the exception of NGC 6765 (062.4+09.5) for which the V magnitude is from Napiwotzki & Schönberner (1995).

The interstellar extinction has been determined from the ratio of the radio to Hβ fluxes if good quality radio flux measurements are available. Otherwise the extinction has been derived from the Hα/Hβ ratio. In this case the resulting logarithmic extinction at Hβ has then been divided by 1.17 in order to correct for a systematic difference between the radio and optical extinctions as discussed in Stasińska et al. (1992).

It is well known that the observationally derived distances to the Galactic PNe are not reliable in most cases. This is the principal source of uncertainties while comparing theoretical models to the observations on the HR diagram or other diagrams involving distances. Therefore in this study instead of analysing luminosities, absolute magnitudes, nebular dimensions or ex-

Table 1. Observational data for planetary nebulae with H-deficient central stars.

PN G	name	spec. type	diam.	log n_e	-log F(Hβ)	F(6cm)	Hα/Hβ	B	V	log $S_{H\beta}$	log S_V
000.4−01.9	M 2-20	[WC 6]	6.5	3.76	12.3		1133		16.1	-1.62	-4.40
001.5−06.7	SwSt 1	[WC 10]	1.3	4.00	10.33	130		11.77	11.76	0.18	-2.63
002.2−09.4	Cn 1-5	[WC 4]	7	3.69	11.21	44	391	15.5	15.2	-1.81	-5.16
002.4+05.8	NGC 6369	[WC 4]	38	3.66	11.32	2130	1297	16.99	15.94	-1.81	-5.56
003.1+02.9	Hb 4	[WC 3]	7.25	3.71	11.95	168.5	1252	18.4	>17	-1.27	-4.99
004.9+04.9	M 1-25	[WC 6]	3.2	3.84	11.92	57.5	853	17.9		-1.02	-4.63
006.0−03.6	M 2-31	[WC 4-6]	4	3.53	12.11	51	858			-1.26	
006.8+04.1	M 3-15	[WC 5]	4.5	3.62	12.45	65	1578			-1.17	
007.8−03.7	M 2-34	[WC]	8.5	3.49:	12.9		949			-2.65	
011.9+04.2	M 1-32	[WC 4]	9	3.42	12.2	61		18.3	17.0	-1.89	-5.12
012.2+04.9	PM 1-188	[WC 11]	4					15.42	14.90		
017.9−04.8	M 3-30	[WC 2]	20	2.25	12.29	7	707		17.9	-3.12	-6.56
019.4−05.3	M 1-61	[WC 4]	1.8	3.99:	11.43	97	648	17.1		-0.29	-4.11
019.7−04.5	M 1-60	[WC 4]	2.5	3.90	12.28	48	977			-0.88	
020.9−01.1	M 1-51	[WC 4-6]	13	3.51	13.0	319	2718			-1.53	
027.6+04.2	M 2-43	[WC 7]	1.5	4.00:	13.1	148	5370			0.05	
029.2−05.9	NGC 6751	[WC 4]	20.5	3.36:	11.26	63	450	15.78	15.45	-2.61	-6.03
048.7+01.9	He 2-429	[WC 4]	4.2	3.80	12.91		1596			-1.46	
060.4+01.5	HuDo 1	[WC 11]							18.6		
061.4−09.5	NGC 6905	[WC 2]	40	2.95	10.92	62	318	16.3	15.7	-3.29	-7.09
064.7+05.0	BD+30°3639	[WC 9]	7.7	4.45	10.03	645	398	11.96	12.50	-0.73	-4.17
068.3−02.7	He 2-459	[WC 9]	1.3	3.55:	12.73	64				-0.25	
089.0+00.3	NGC 7026	[WC 3]	20	3.52:	10.90	265	601	15.33	14.20	-1.94	-5.26
096.3+02.3	K 3-61	[WC 4-6]	6	3.14:	13.2	14	1216	>15.9	>14.8	-2.21	<-3.61
120.0+09.8	NGC 40	[WC 8]	48	3.23	10.66	495	494	11.82	11.58	-2.55	-5.05
130.2+01.3	IC 1747	[WC 4]	13	3.56	11.49	110:	608	15.8	15.4	-2.12	-5.34
144.5+06.5	NGC 1501	[WC 4]	52	3.22	11.28	200:		15.17	14.39	-3.01	-6.05
146.7+07.6	M 4-18	[WC 11]	3.75	3.68:	11.89	20	488	14.22	13.96	-1.61	-3.83
161.2−14.8	IC 2003	[WC 3]	9	3.77:	11.19	48	357	14.7	15.0	-2.07	-5.35
189.1+19.8	NGC 2371-72	[WC 3]	54	2.99:	10.99		327	14.48	14.85	-3.56	-6.97
243.3−01.0	NGC 2452	[WC 2]	18.8	3.34	11.49	55	412	17.71		-2.78	-6.84
278.1−05.9	NGC 2867	[WC 2]	14	3.39	10.58	252	386	16.62		-1.75	-6.30
278.8+04.9	PB 6	[WC 2]	11	3.34	11.87	30	459	17.4	17.6	-2.61	-6.29
285.4+01.5	Pe 1- 1	[WC 4-5]	3	4.04	12.26		1154			-08	
286.3+02.8	He 2- 55	[WC 3]	18	2.60	12.5		481	17.6	17.4	-3.68	-6.65
291.3−26.2	Vo 1	[WC 11]		>5.00	13.17			16.7	15.8		
307.2−03.4	NGC 5189	[WC 2]	147	2.69:	10.52	413	467	14.92		-3.56	-7.46
309.0−04.2	He 2- 99	[WC 9]	17	3.07:	11.91	18:	581	14.22	14.00	-2.82	-5.06
309.1−04.3	NGC 5315	[WC 4]	6	3.90:	10.42	480	465	14.58	14.40	-0.66	-4.51
321.0+03.9	He 2-113	[WC 11]	1.3	4.24:	11.83	115	697	12.97	12.28	-0.14	-1.81
324.0+03.5	PM 1-89	[WC 4]	27					16.2			
327.1−02.2	He 2-142	[WC 9]	3.5	4.50:	11.84	65	998	15.88	15.15	-0.90	-3.73
332.9−09.9	He 3-1333	[WC 11]	1.84	>4.70	12.02	26	571	12.13	11.50	-0.97	-2.10
336.2−06.9	PC 14	[WC 4]	7	3.41	11.73	30	522	17.2	16.5	-1.99	-5.38
337.4+01.6	Pe 1- 7	[WC 9]	< 5	4.74:	12.51	117	2056	17.9	16.7	>-1.01	>-3.90
352.9+11.4	K 2-16	[WC 11]	23					13.18	12.75		
355.2−02.5	H 1-29	[WC 4-6]		3.67	12.64		871				
355.9−04.2	M 1-30	[WC 7]	3.5	3.73	11.77	31	567	16.6	16.4	-1.36	-4.69
358.3−21.6	IC 1297	[WC 3]	7	3.45	10.95		344	14.8	14.2	-1.69	-4.88
042.5−14.5	NGC 6852	PG 1159	28		11.7	20	242	17.70	17.90	-3.70	-7.62
046.8+03.8	CTSS 3	PG 1159	600					17.98	17.78		
062.4+09.5	NGC 6765	PG 1159	40	3.05	11.90		430		17.8[b]	-3.90	-7.62
094.0+27.4	K 1-16	PG 1159	110		12.00		250:	14.74	15.08	-5.35	-7.81
104.2−29.6	Jn 1	PG 1159	313		11.48		350	15.72	16.13	-5.50	-8.94
118.8−74.7	NGC 246	PG 1159	245	2.30	10.53	>165	312	11.60	11.96	-4.47	-7.17
130.9−10.5	NGC 650-51	PG 1159	70	2.55	10.68	>102	388	16.1	15.9	-3.28	-7.44
149.7−03.3	IsWe 1	PG 1159	780					16.45	16.56		
164.8+31.1	JnEr 1	PG 1159	384		11.27			16.53	16.83		
205.1+14.2	A 21	PG 1159	615	2.27	10.4	327:	224	15.67	15.99	-5.05	-9.51
258.0−15.7	Wray 17- 1	PG 1159	82	3.00:	11.4		309			-4.40	
274.3+09.1	Lo 4	PG 1159	48	2.95	12.6		277	22.0	20.5	-5.23	-9.26
286.8−29.5	K 1-27	O(He)	46		12.7		311:		16.7	-5.19	-7.62
291.4+19.2	ESO 320-28	O(He)	32		12.8		376:			-4.76	
081.2−14.9	A 78	Of-WC(C)	103		12.04		294	13.02	13.21	-5.30	-6.98
208.5+33.2	A 30	Of-WC(C)	119	2.85:	12.19		230	14.32	14.38	-5.61	-7.60

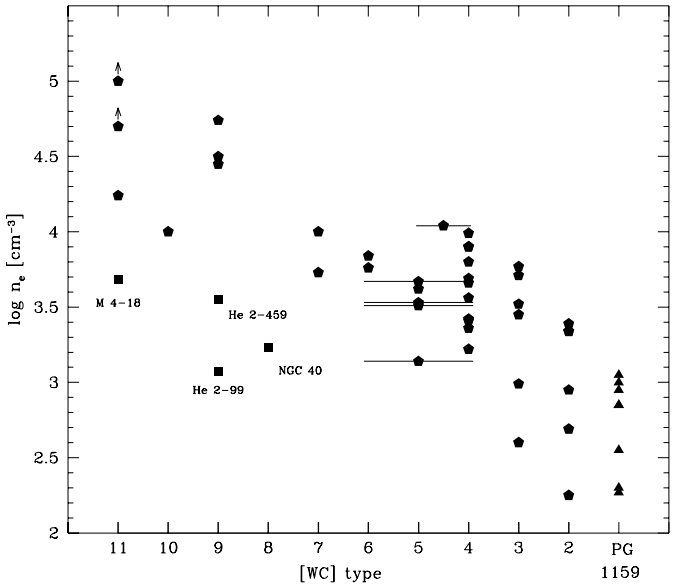

Fig. 1. Nebular electron density versus spectral type of H-deficient PNNi.

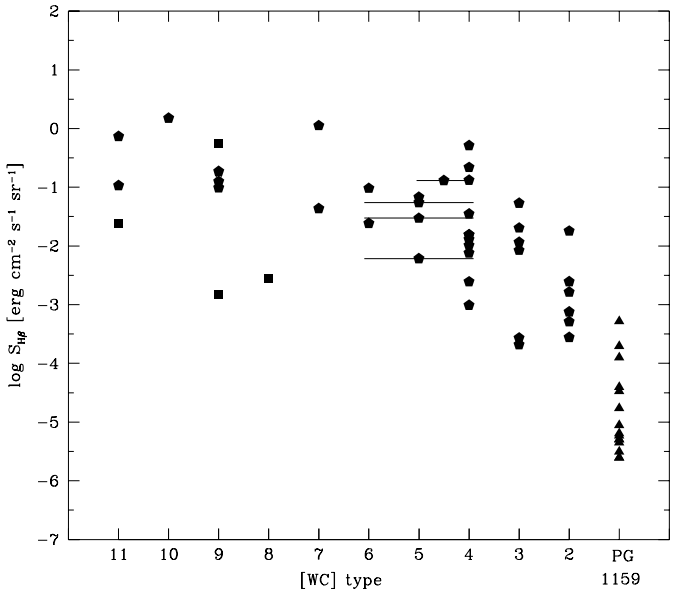

Fig. 2. Hβ surface brightness versus spectral type of H-deficient PNNi.

pansion ages we investigate parameters which do not involve distances.

Thus we use $n_{\rm e}$ derived from forbidden line ratios as an indicator of the nebular age. Another parameter which we use in our investigations is the Hβ surface brightness which is defined as

$$S_{\rm H\beta} = F({\rm H}\beta)/(\pi\theta^2)$$

where $F({\rm H}\beta)$ is the Hβ nebular flux corrected for extinction and θ is the nebular angular radius. Similarly as $n_{\rm e}$, $S_{\rm H\beta}$ also measures the nebular age but it is derived from other independent observational measurements. The third parameter we are exploring is $S_{\rm V}$ defined as

$$S_{\rm V} = F_{\rm V}/(\pi\theta^2)$$

where $F_{\rm V}$ is the stellar flux (corrected for extinction) in the V band. $S_{\rm V}$ has been proposed in Górny et. al. (1997a) and is closely related to the parameter f introduced in Tylenda & Stasińska (1989). It combines information on the evolutionary advancement of the central star with the expansion stage of the nebula. The value of $S_{\rm V}$ decreases by many orders of magnitude during the PN phase (much more than $n_{\rm e}$ and $S_{\rm H\beta}$) and therefore it is a very useful parameter for distinguishing young, newly formed objects from evolved ones.

The values of $S_{\rm H\beta}$ and $S_{\rm V}$ calculated for our sample of H-deficient PNNi are given in Table 1 in Columns (11) and (12), respectively. In both cases the units are erg cm^{-2} s^{-1} sr^{-1}.

3. Evolutionary sequence of H-deficient PNNi

Fig. 1 plots $n_{\rm e}$ versus the [WC] subclass of the central star. The last bin, labelled PG 1159, includes other H-deficient PNNi. Later on in this paper all the H-deficient PNNi which have not been classified as [WC] will be called, for simplicity, as PG 1159-type.

Fig. 1 confirms the finding of Acker et al. (1996) that the nebular density tends to decrease as one goes from [WC 11] to [WC 2]. As can be seen from Fig. 1, the PG 1159-type objects clearly follow the sequence in the sense that on average they have nebulae of lower density than the earliest [WC] PNNi. Four [WC] objects have been marked with filled squares in Fig. 1. These are late-[WC] PNNi having significantly lower $n_{\rm e}$ than the other objects of this class. Acker et al. (1996) have suggested that these low density, late [WC] objects can have a different evolutionary status from the rest of the [WC] PNNi. We return to this point at the end of this section.

Fig. 2 shows the Hβ surface brightness plotted against the central star spectral type. The notation is the same as in Fig. 1. Similarly as $n_{\rm e}$ in Fig. 1, $S_{\rm H\beta}$ also decreases while going from late-[WC] to early-[WC] and PG 1159.

The same evolutionary sequence, even more pronounced than those in Figs. 1 and 2, can be seen in Fig. 3 which plots $S_{\rm V}$ versus the PNN spectral type.

Simple evolutionary considerations show that all the observational parameters investigated in this section, i.e. $n_{\rm e}$, $S_{\rm H\beta}$ and $S_{\rm V}$, decrease as the nebula and its central star evolve with time. Therefore Figs. 1–3 give observational evidence that the general evolutionary sequence of the H-deficient PNNi is: late-[WC], early-[WC], PG 1159. This sequence is most clearly seen in Fig. 3 exploring $S_{\rm V}$. As noted in Sect. 2, $S_{\rm V}$ is a parameter easily distinguishing between young and old objects.

The above evolutionary sequence is the same as that inferred from spectroscopic studies of the H-deficient nuclei (e.g. Hamann 1997). It is also worth noting that infrared studies of the [WC] type PNe suggest that the early-[WC] PNNi evolve from the late types (Górny et al. 1997b).

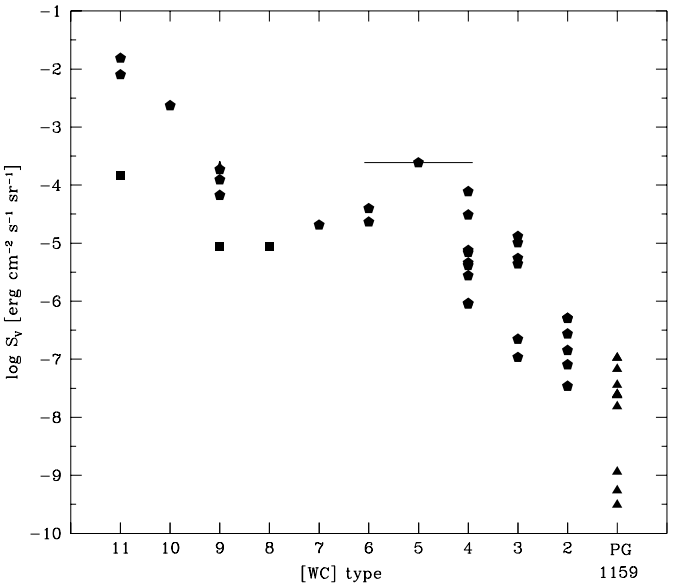

Fig. 3. $S_{\rm V}$ versus spectral type of H-deficient PNNi.

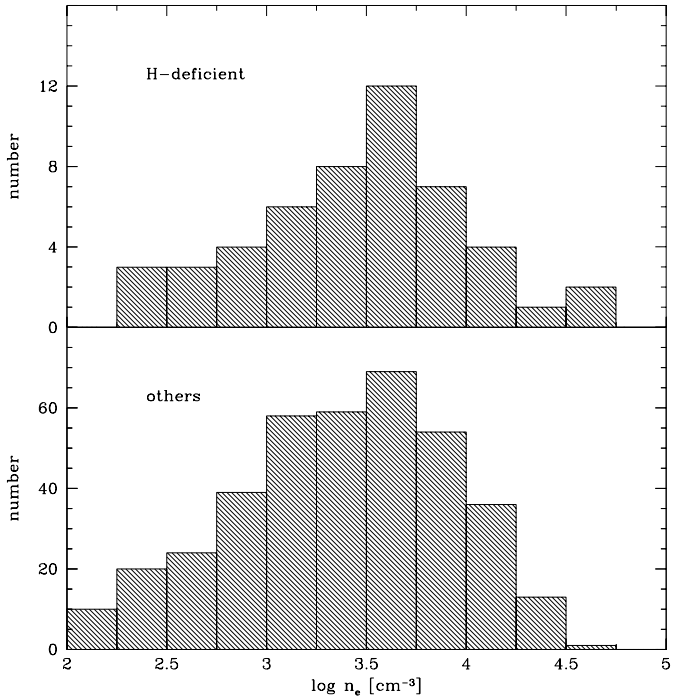

Fig. 4. Histograms of nebular electron density for PNe with H-deficient central stars and other PNe.

It should however be stressed that the evolutionary sequence resulting from the above consideration, i.e. late-[WC], early-[WC], PG 1159, should be regarded as a general evolutionary scheme for most of H-deficient PNNi. The available observational data are not good enough to investigate the evolutionary status of individual objects. Especially that we are lacking reliable theoretical evolutionary models for H-deficient PNNi. Therefore we cannot claim that all the H-deficient PNNi exactly follow the above sequence. In fact, from the discussion in Sect. 5.2, we expect that in the PG 1159 population there might be objects that have avoided evolution through the [WC] sequence.

Four objects of late [WC] have been distinguished in Fig. 1 (filled squares) as they have significantly lower $n_{\rm e}$ and do not seem to fit to the general evolutionary sequence, as suggested by Acker et al. (1996). However, in Fig. 2 and particularly in Fig. 3 these objects fit much better to the general trend. The electron density has been derived from the [S II] lines and may refer to less dense nebular regions in these objects ([S II] lines are collisionally de-excited at high $n_{\rm e}$). Thus we conclude that the suggestion of Acker et al. (1996) that the discussed objects have a different evolutionary status is too far reaching. These central stars seem, however, to evolve somewhat slower than the rest of the population. This can be inferred from the fact that they tend to occupy lower parts of the distributions in Figs. 1–3. Normally a slowly evolving PNN is interpreted as having a low mass. It seems that it is a likely interpretation in the case of the four late-[WC] PNNi marked with squares in Figs. 1–3. However one has to remember that the presently avaiable PNN models, even those burning He, have been calculated with H-rich envelopes and therefore they do not correspond to the [WC] PNNi. For a [WC] PNN the effective photosphere is formed in the wind and it is the wind density which is the primary factor determining photospheric parameters and thus the observed spectral type. It is not clear if the PNN mass is the only important factor determining the evolution of the wind density in the [WC] phase.

4. PNe with H-deficient central stars versus other PNe

In this section we compare the PNe having H-deficient nuclei with the rest of the Galactic PN population. The latter sample, for simplicity named "others", includes all the PNe whose central stars have not been found to be H-deficient. Most of the objects in this sample have H-rich PNNi although it cannot be excluded that some of them have yet undetected H-poor central stars. The observational data base for the others comes from the same sources as Table 1.

Fig. 4 compares the distribution of the nebular densities in the case of the H-deficient PNNi with that obtained for the others. The same but for $S_{{\rm H}_\beta}$ and $S_{\rm V}$ is shown in Figs. 5 and 6, respectively. Objects for which only lower limits are known have been excluded from the histograms.

As can be seen from Figs. 4–6, the distributions for both samples are very similar. Statistical tests of Kolmogorov–Smirnov and of Wilcoxon confirm that there is no statistically important difference between them.

Let us pay more attention to the parts of the distributions corresponding to dense and high surface brightness objects, i.e. $\log n_{\rm e} > 3.5, \log S_{{\rm H}_\beta} > -2.0, \log S_{\rm V} > -5.5$. These parts are expected to be most complete and least subject to observational selection effects. As it can be seen from Figs. 4–6 they look very much the same for both samples. The ratio of the H-deficient PNN to the others for $\log n_{\rm e} > 3.5$ is 15.6%. For the whole samples this ratio is 13.0%. For objects with $\log S_{{\rm H}_\beta} > -2.0$ the H-deficient proportion is 8.9% against 7.0% for the entire

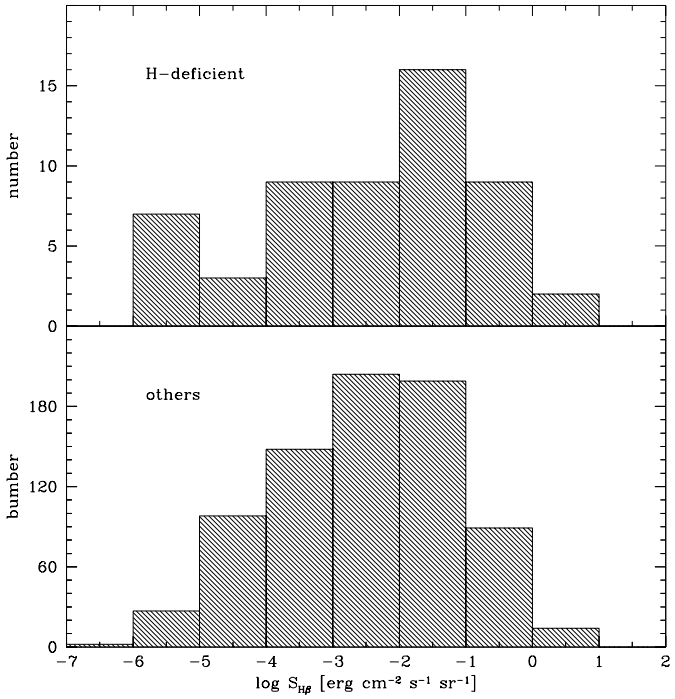

Fig. 5. Histograms of Hβ surface brightness for PNe with H-deficient central stars and other PNe.

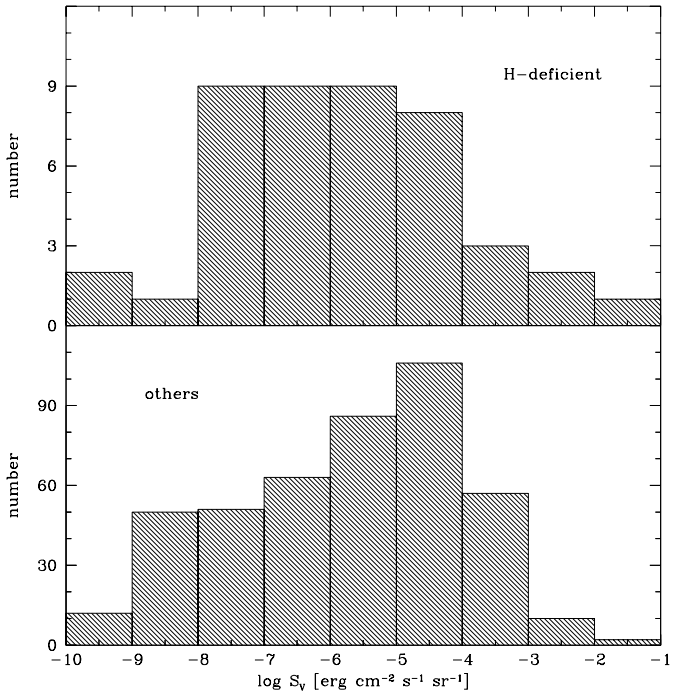

Fig. 6. Histograms of $S_{\rm V}$ surface brightness for PNe with H-deficient central stars and other PNe.

samples. In the case of $\log S_{\rm V} > -5.5$ the respective figures are exactly 10.1% and 10.1%. This shows that the H-deficient PNNi are not underpopulated (neither overpopulated) among dense, high surface brightness PNe. In other words, the H-deficient stars become observable as PNNi at a similar evolutionary (expansion) stage of the nebulae as the others. This is an important conclusion for the discussion later on in this paper.

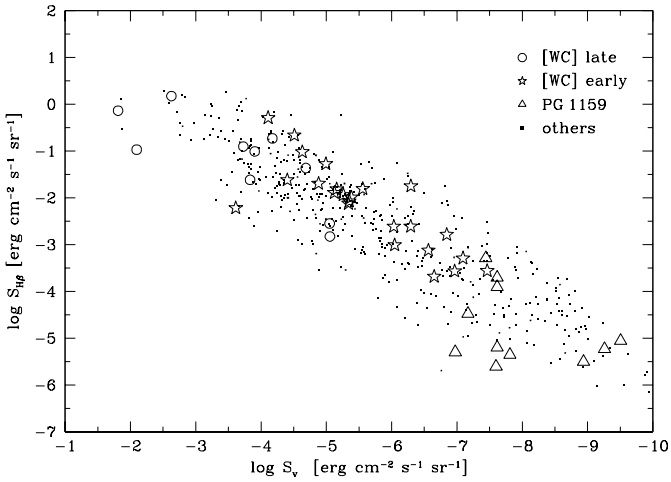

Fig. 7. $S_{\rm H\beta}$ versus $S_{\rm V}$ for PNe with H-deficient central stars and other PNe.

Fig. 7 plots $S_{\rm H\beta}$ versus $S_{\rm V}$ for the objects from both samples. As shown in Górny et al. (1997a) and Stasińska et al. (1997) this diagram is useful for studying the evolution of PNNi. The objects evolve from the upper-left to the lower-right of the diagram. High mass, fast evolving PNNi are expected to be observed along the upper-right portion of the distribution.

The H-deficient sample presented in Fig. 7 has been devided into three subsamples, i.e. late-[WC] ([WC 11–7]), early-[WC] ([WC 6–2]) and PG 1159 (non-[WC]). Thus the general evolutionary sequence of the H-deficient PNNi, as discussed in the previous section, can be seen from Fig. 7 as well.

The main feature of the diagram displayed in Fig. 7 is that the distribution of the H-deficient PNNi is very much the same as that of the others. There is no region in the diagram where the H-deficient PNNi would be evidently lacking or appearing more often in comparison to the others. It can thus be concluded that the general trend and the rate of evolution of the objects are the same for both samples.

5. Late He-shell flash scenario

Theoretical evolutionary PNN models predict that in some cases an initially H-burning PNN after having extinguished its H-burning shell and while being on the cooling phase can enter in a He-shell flash (Schönberner 1979, Iben et al. 1983). Convection which develops above the He-burning shell cuts into the remaining H-rich envelope. Hydrogen while being brought down to the base of the convective envelope is burnt. Helium and carbon are brought up to the surface. The star quickly brightens, expands and sets up close to the AGB. Then it repeats the PNN evolution, now as a He-burner having, most probably, a H-deficient atmosphere. Iben (1984) estimates that 5–9% of the PNN population is expected to pass through this evolutionary path.

The very late He-shell flash scenario is very appealing when trying to explain the origin of the H-deficient PNNi (Schönberner & Blöcker 1992; Iben & MacDonald 1995). First of all it explains easily the observed surface abundances (roughly 50% of He and 50% of C, by mass). Statistics also seems to agree. Tylenda (1996) estimates that about 6.5% of the PN population have [WC] type nuclei. This should be considered as a lower limit for the H-deficient PNN population, thus in agreement with the Iben's estimate.

However, this scenario inevitably implies that H-deficient PNNi should be observed preferentially in old, extended nebulae. This is of course the case of the PG 1159 type objects but not of the [WC] PNNi. As has been discussed in Sect. 3 the late-[WC] PNNi usually are observed to have dense, high surface brightness nebulae (cf. Figs. 1–3). As concluded in Sect. 4 the histograms in Figs. 4–6 show that the youngest nebulae (i.e. having the highest values of $n_{\rm e}$, $S_{\rm H_\beta}$ and $S_{\rm V}$) with H-deficient nuclei are of similar evolutionary age as those with other (mostly H-rich) PNNi. One may argue that the [WC] PNNi are more massive than the others (e.g. Heap 1982). Their evolution before the late He-shell flash would then be fast and the second passage across the PNN region would occur in relatively compact nebulae. However, a detailed study of nebular abundances and morphologies in Górny & Stasińska (1995) and Górny (2000) shows that the [WC] phenomenon does not preferentially occur in massive stars. The same conclusion can also be drawn from the observed distribution of the PNe in the Galaxy (Acker et al. 1996).

5.1. Models versus observations

We have attempted to make a quantitative comparison between the late He-shell flash scenario and the observations of the H-deficient PNNi and their nebulae. In this point of the present study we follow the general approach elaborated in our previous works devoted to comparison of theoretical evolutionary models with the PN observations (e.g. Górny et al. 1994, Stasińska & Tylenda 1994, Górny et al. 1997a, Stasińska et al. 1997). The main point of our approach is that instead of trying to determine absolute values (e.g. PNN luminosity, effective temperature or PN radius) we use parameters which are easy to derive from observations and which are distance independent. Then from theoretical modelling of a given scenario we obtain values of the same parameters for direct comparison with the observations. In the present study the comparison is done in the $S_{\rm H_\beta}$ – $S_{\rm V}$ plane.

As the base of our simulations of the late He-shell flash scenario we have adopted the 0.6 M$_\odot$ PNN model from Iben at al. (1983) (in fact it is the only late He-shell flash model available in literature for our purpose). We also adopt that the PN is formed when the star for the first time leaves the AGB and starts evolving fast towards the PNN domain. This takes place at $t \simeq -10\,000$ yrs in the notation of Fig. 1 of Iben et al. (1983) when $\log T_{\rm eff} \simeq 3.7$. Thus we take this moment as the zero age of the PN. The PNN initially evolves as a H-burner and at the PN age of 28 600 yrs it experiences a late He-shell flash. The star quickly returns almost to the AGB and repeats its evolution through the PNN domain now as a He-burner. During this phase the star is expected to be H-deficient.

The PNN model of Iben et al. (1983) comes from calculations done for the abundances relevant to the Magellanic Clouds (Z = 0.001). This is probably the main reason why during the initial H-burning phase it evolves much slower than 0.6 M$_\odot$ H-burning models done by other authors for the Population I abundances (see Schönberner 1989). Indeed our preliminary calculations show that the PNN evolution in the H-burning phase of Iben at al. is not compatible with the observed distribution of the others in Fig. 7. Therefore in order to have a PNN model more relevant to the Galactic objects we have accelerated the evolutionary speed of the PNN model of Iben et al. by factor 3. In this way we have obtained a PNN model which in the H-burning phase evolves more or less like the 0.598 M$_\odot$ model of Schönberner (1981) and the 0.605 M$_\odot$ model of Blöcker (1995). Thus in our modified PNN model the late He-shell flash begins about 9500 yrs after the PN formation.

In order to be able to place the model evolution on the $S_{\rm H_\beta}$ – $S_{\rm V}$ diagram we have to adopt a model nebula. We take a simple, standard PN being a spherically symmetric shell of 0.2 M$_\odot$. The PN mass is kept constant during its evolution. The PN expands during the H-burning phase at a constant velocity of 20 km s^{-1}. At the begining of the He-burning phase we have increased the expansion velocity up to 30 km s^{-1}. These values correspond to the mean expansion velocities for the others (presumably mostly H-burning) and for the [WC] type PNe, respectively (Tylenda & Górny 1993; Górny & Stasińska 1995). The filling factor of nebular shell ε is adopted to be 0.5 and is kept constant with time. The model PN is ionized by the PNN assumed to radiate as a black body. Certainly the black body is a crude approximation of the PNN spectrum. However, what we need to calculate is the extension of the H$^+$ region in the nebula which depends on the total number of ionizing photons rather than on their exact spectral distribution. In this respect the black body is expected to be a reasonable approximation as can be inferred from Leuenhagen et al. (1996). These authors have obtained a good agreement between the Zanstra (black body) temperature, T$_Z$(HI), and their values of T$_{2/3}$ (referring to the radius when the observed PNN radiation is mostly formed). Having derived the hydrogen ionization structure of the model nebula we can calculate the model values of $S_{\rm H_\beta}$ and $S_{\rm V}$.

The results of the above described model (later on referred to as the standard model) are displayed and compared to the observations in Fig. 8. The dashed curve shows the model evolution for the H-burning phase. The dotted curve represents the fast evolution during the thermal pulse. The full curve corresponds to the He-burning phase after the born again AGB. Large symbols represent H-deficient PNNi, small ones – the others.

As can be seen from Fig. 8 the dashed curve, representing the H-burning phase, can be considered as a typical model for the whole population of PNe. It fits quite well the observed positions of the others. Obviously it does not reach the lower-right part of the observed distribution in Fig. 8 as its evolution towards faint objects has been interrupted by the He-shell flash. After the

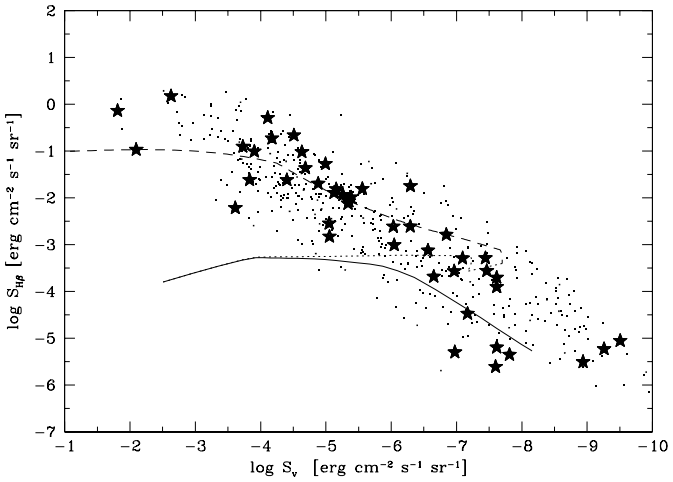

Fig. 8. Comparison of the modelled evolution in the very late He-flash scenario with the observations. Large symbols – H-deficient PNNi, small symbols – the others. Dashed, dotted and full lines show H-burning, thermal pulse and born-again He-burning phases, respectively.

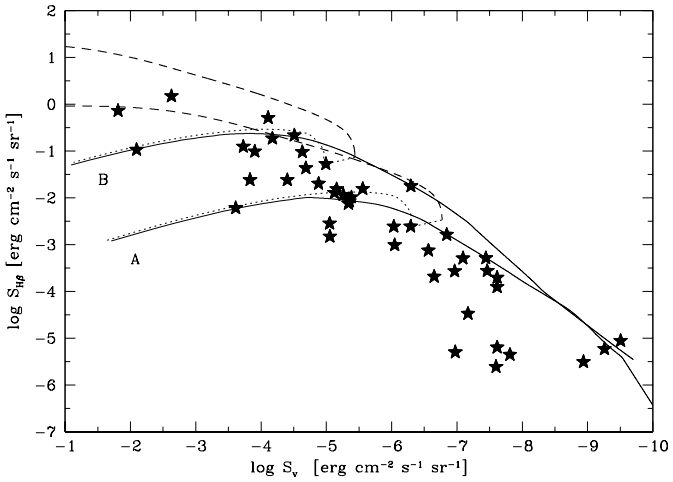

Fig. 9. The very late He-flash scenario calculated adopting PN mass of 1.0 M$_\odot$ (A) and 10.0 M$_\odot$ (B). Other parameters as in the standard model. The same notation as in Fig. 8. Symbols – observed H-deficient PNNi.

flash, when the model returns to the PN region as a He-burner, it should represent the evolution of H-deficient PNNi. However, as can be seen from Fig. 8, it is not the case for the majority of the observed H-deficient objects. The full curve matches the lower-right part of the observed distribution occupied mainly be the PG 1159 objects. However, in the case of the [WC] objects the full curve cannot be considered as reproducing the observed positions. The model predicts that there should be no H-deficient PNNi for nebulae with $\log S_{\mathrm{H}\beta} \gtrsim -3.5$ whereas the [WC] objects in the bulk do have $\log S_{\mathrm{H}\beta} \gtrsim -3.5$.

In order to get a better agreement between the model and the observations one can consider larger masses of the model nebula and/or higher masses of the central star. An increase in the PN mass would obviously increase $S_{\mathrm{H}\beta}$ and the full curve in Fig. 8 would be shifted towards the region occupied by the late-[WC] PNNi. A higher PNN mass would result in a faster evolution of the central star and the He-burning phase would begin when the nebula is smaller and denser, i.e. while having higher $S_{\mathrm{H}\beta}$.

Fig. 9 shows the results of the calculations done with the same model parameters as in our standard model except the PN mass which is here 1.0 M$_\odot$ and 10.0 M$_\odot$. The He-burning tracks in Fig. 9 are in better agreement with the observed positions of the H-deficient PNNi. However, in order to get a reasonable agreement of the model with the late-[WC], high surface brightness objects the model nebula as massive as 10.0 M$_\odot$ has to be adopted. This is unacceptably large for a PN. Moreover, as can be seen from Fig. 9, such a massive nebula evolves above the positions of the early-[WC] and PG 1159 objects.

We cannot explicitly increase the mass of the central star in our model calculations as the 0.6 M$_\odot$ model of Iben et al. (1983) is the only available PNN model with a late He-shell flash. However, we can, to some extend, simulate the evolution of a more massive central star by increasing the evolutionary speed of the model PNN. Although a higher PNN mass generally implies a higher PNN luminosity and the evolution to higher effective temperatures it is the evolutionary speed which has the strongest dependence on the PNN mass (e.g. Iben & Renzini 1983). We have carried out calculations in which the central star evolves 5 and 10 times faster than the original model of Iben et al., i.e. 1.7 and 3.3 faster than in our standard model. Judging from the H-burning PNN models (Schönberner 1981, Blöcker 1995, see also Iben & Renzini 1983) an increase by factor 1.7 and 3.3 in the evolutionary speed would correspond to an increase in the PNN mass by 5% and 13%, respectively. Obviously this is to be considered as a crude estimate. In the case of [WC] PNNi we deal with He-burning and very intense mass loss and the dependence of the evolutionary time scale on the PNN mass may be different.

The results of the calculations in which the PNN evolves faster than in the standard one (other model parameters remain the same) are displayed in Fig. 10. As can be seen from Figs. 9 and 10 an acceleration of the evolution of the central star has a very similar effect as an increase in the nebular mass. The full curves in Fig. 10 fit the positions of the [WC] objects better than in Fig. 8. A reasonable representation of the observed positions of the late-[WC] objects is provided by the PNN evolving 3.3 times faster than in our standard model. According to our crude estimates this would correspond to the PNN mass of 0.68 M$_\odot$. From the point of view of the expected parameters in the PN population this solution is certainly more acceptable than the 10.0 M$_\odot$ PN displayed in Fig. 9.

The main conclusion which can be drawn from our modelling presented in Figs. 8–10, is that if the observed H-deficient PNNi are to be interpreted as resulting from the late He-shell flash than this phenomenon should preferentially occur in objects with high PNN mass and/or large PN mass. Low mass and typical PNe should rather avoid it.

The question that now arises is: in the observed PN population, do we have enough "potential progenitors" of the H-

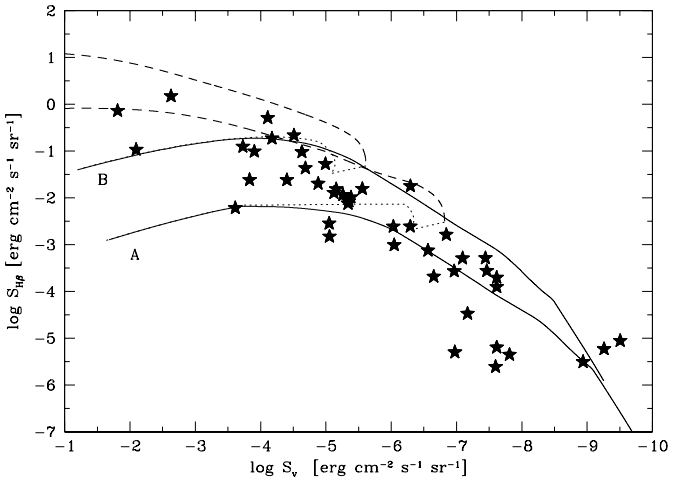

Fig. 10. The very late He-flash scenario modified by adopting the central star evolution to be 1.7 times (A) and 3.3 times (B) faster than in our standard model. Other parameters as in the standard model. The same notation as in Fig. 8.

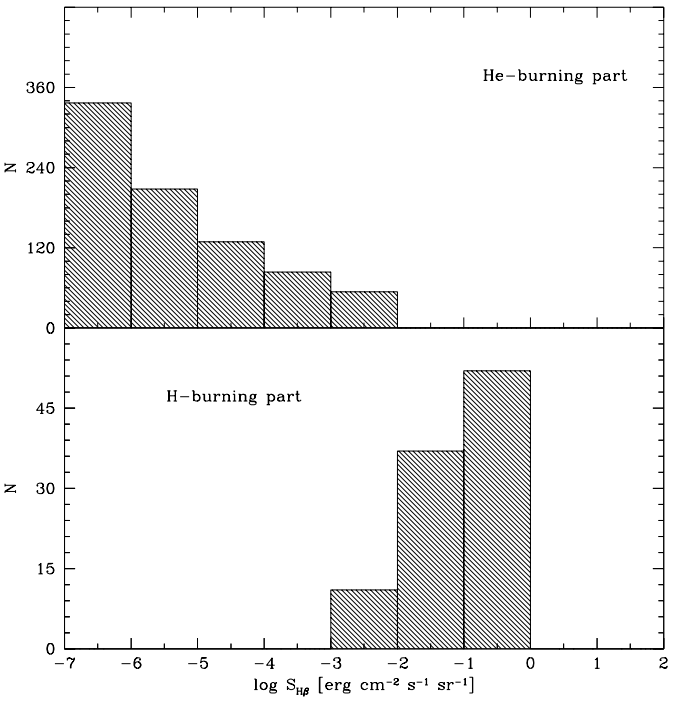

Fig. 11. Expected distributions in $S_{\mathrm{H}\beta}$ of the H-deficient PNNi and their H-burning progenitors from the model with the PN mass of 1.0 $\mathrm{M}_{\odot}$. Other parameters as in our standard model. Histograms have been normalized to 100 objects in the H-burning sample.

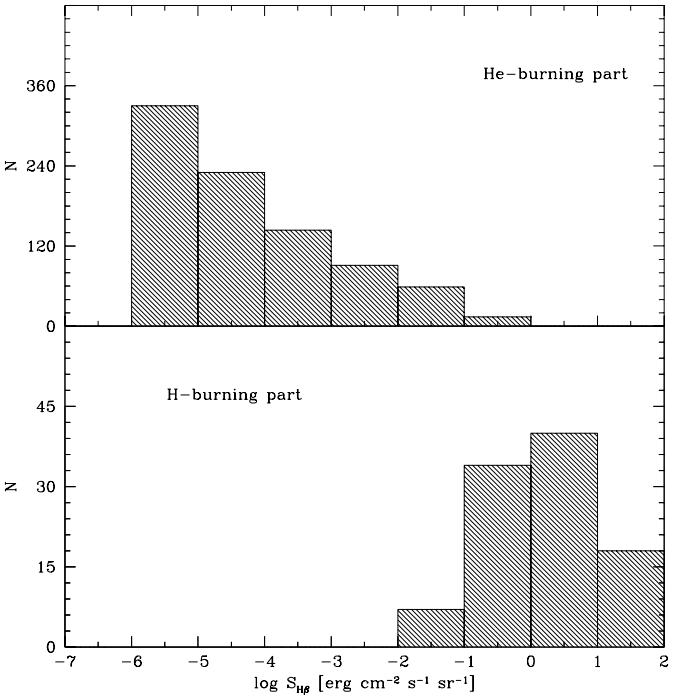

Fig. 12. Expected distributions in $S_{\mathrm{H}\beta}$ of the H-deficient PNNi and their H-burning progenitors from model with the central star evolving 3.3 times faster than in our standard model. Other parameters the same as in the standard model. Histograms have been normalized to 100 objects in the H-burning sample.

deficient PNNi if they are supposed to be preferentially massive objects? As it is evident from Figs. 8–10 these progenitors should be observed among the H-rich PNNi brighter in $S_{\mathrm{H}\beta}$ than the brightest H-deficient objects. This seems to be in conflict with the finding of Sect. 4 that the H-deficient and the H-rich populations are not distinguishable in the $S_{\mathrm{H}\beta}$ histogram, including the brightest portions of the distributions. Especially that, as can be seen from Figs. 9 and 10, for the models fitting reasonably well the [WC] objects the dashed curves (representing the H-burning) pass at upper bounds of the PN population, where only a few objects are observed (see positions of the others in Fig. 7 or 8).

In order to investigate this point we have produced expected distributions in $S_{\mathrm{H}\beta}$ of the H-deficient PNNi and their H-burning progenitors from our models. Assuming that the number of objects in a particular $S_{\mathrm{H}\beta}$ bin is proportional to the time spent by the model within this bin we have obtained histograms presented in Figs. 11 and 12. For each model the histograms have been normalized to 100 objects in the H-burning sample.

Figs. 11 and 12 present the results from two models only, i.e. the 1.0 $\mathrm{M}_{\odot}$ PN model displayed in Fig. 9 and the 3.3 times faster (than the standard one) evolving model from Fig. 10. Obviously the derived histograms look somewhat different and are shifted to higher or lower surface brightnesses, depending on the model used. However in all cases they show the same feature: the H-burning progenitors of the H-deficient PNNi are expected to be 2-3 orders of magnitude brighter in $S_{\mathrm{H}\beta}$ than the brightest H-deficient PNNi. From all our models it results that the number of the H-deficient PNNi in the first two (three) brightest bins in $\log S_{\mathrm{H}\beta}$ should be comparable to (twice larger than) the number of the H-burning progenitors. The progenitors should be at least as bright in $S_{\mathrm{H}\beta}$ as the brightest H-deficient stars.

In our sample of the H-deficient stars we have 11 (27) objects which have $\log S_{\mathrm{H}\beta}$ greater than -1.0 (-2.0) (see Table 1 and Fig. 5). Thus in the PN population we can expect to have about

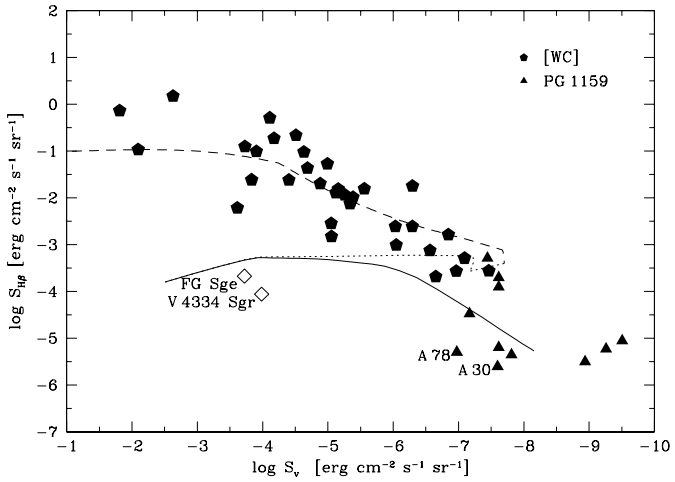

Fig. 13. Comparison of observed positions of FG Sge, V4334 Sgr, A 30 and A 78 with predictions from our standard model of the late He-shell flash. The same notation of the model as in Fig. 8.

10–13 H-burning progenitors having log $S_{\mathrm{H}\beta} \gtrsim 0.0$. However the number of the so bright PNe in the observed population should be much larger. The point is that only a small part of the H-burning PNNi has a chance to undergo a He-shell flash during its life time. According to Iben (1984) only 9% of the PNNi are expected to experience a very late He-shell flash. Thus we should observe at least 100 PNe with log $S_{\mathrm{H}\beta} \gtrsim 0.0$ and many of them should be as bright as log $S_{\mathrm{H}\beta} = 2.0$. In the observed sample of 781 PNe (for which we have been able to determine $S_{\mathrm{H}\beta}$) there are only 14 objects with $0.0 < \log S_{\mathrm{H}\beta} < 1.0$ and none for log $S_{\mathrm{H}\beta} > 1.0$. Therefore our final conclusion is that the H-deficient PNNi, at least of the [WC] type, in their majority do not result from the very late He-shell flash (or born again AGB).

5.2. Observed cases of the late He-shell flash in PNNi

The above conclusion may seem to be contradicted by the fact that there are a few PNe for which we have strong observational arguments that their central stars have indeed experienced a late He-shell flash. As we show below this is not the case and in fact the analysis of the observational data for these objects reinforces the conclusion drawn in the previous subsection.

Fig. 13 shows the $S_{\mathrm{H}\beta} - S_{\mathrm{V}}$ diagram in which the observed positions of the objects discussed in this subsection are compared with other H-deficient PNNi and the predictions from our standard model of the late He-shell flash.

As discussed in Iben et al. (1983) the central stars of A 30 and A 78 have very probably suffered from a late He-shell flash. These two large, low surface brightness PNe display in their central parts H-deficient material (Hazard et al. 1980; Jacoby & Ford 1983) which have apparently been ejected from the central star well after the main nebula had been formed (Reay et al. 1983). A low expansion velocity of the H-deficient nebular knots (22-25 km s^{-1} – Reay et al. 1983) compared to the wind velocity from the central star (4000 km s^{-1} – Leuenhagen et al. 1993) strongly suggests that the knots have been ejected while the central star had giant dimensions. As can be seen from Fig. 13 the positions of A 30 and A 78 in the $S_{\mathrm{H}\beta} - S_{\mathrm{V}}$ diagram are consistent with the expected evolution after a late He-shell flash in a typical PNN.

A 58 is an object similar to the two discussed above. It is an extended, faint PN. Its central star, V605 Aql, had a nova-like outburst in 1919 which can be interpreted as a thermal pulse due to a He-shell flash (e.g. Bond et al. 1993). At present the central parts of A 58 show nebular emission from H-deficient material while the central star seems to display [WC] characteristics (Seitter 1989). The lack of reliable measurements of the Hβ flux from A 58 and of the brightness of its central star has prevented us from placing this object in Fig. 13. However, it is clear that A 58 has a very low surface brightness (Abell 1966, Ford 1971).

FG Sge is probably the best documented case of a PNN which has recently experienced a He-shell flash. From an analysis of the observed evolution of its visual brightness Blöcker & Schönberner (1997) have concluded that FG Sge has a mass of 0.61 M$_\odot$. FG Sge is at present too cool to be able to ionize the surrounding PN, He 1-5. However the observed spectrum of He 1-5 can easily be accounted for by a recombining nebula (Tylenda 1980). The present position of the object in the $S_{\mathrm{H}\beta}$ – S_{V} diagram is shown in Fig. 13. The observational data for the nebula and the central star have been taken from Hawley & Miller (1978) and Yudin & Tatarnikov (1999), respectively. As can be seen from Fig. 13 this position fits nicely with the predictions of our standard model during the thermal pulse.

V4334 Sgr, also known as the Sakurai's object, is presumably another example of a PNN undergoing a late He-shell flash (e.g. Kerber et al. 1999). The star is surrounded by an extended faint PN investigated recently by Kerber et al. (1999) and Pollacco (1999). Using the results from these studies and the V brightness of V4334 Sgr from Yudin & Tatarnikov (1999) we have derived the present position of the object in Fig. 13 which is quite close to that of FG Sge.

The general conlcusion from Fig. 13 is that the observational data for A 30, A 78, FG Sge and V4334 Sgr are indeed consistent with the idea that these object have suffered (or are suffering) from a late He-shell flash. A better agreement between the model and the observational data in Fig. 13 would be obtained if the He-shell flash occured a bit later than in our standard model. The position of A 58 in Fig. 13 cannot be determined but judging from the low surface brightness of the nebula it should also agree with the model predictions.

From the observational data for the above objects it can be clearly shown that none of them has a real chance to evolve towards typical PNe with [WC] PNNi. The two objects which have recently experienced a late He-shell flash, i.e. FG Sge and V4334 Sgr, have nebulae with log $S_{\mathrm{H}\beta} < -3.5$. In course of time their surface brightnesses will decrease. S_{V} will also decrease due to the expansion of the nebulae and the expected decrease of the V magnitude of the central stars when recovering from the thermal pulse. Thus, as can be seen from Fig. 13, these objects will evolve directly to the region occupied by the

PG 1159 objects. They have no chance to pass through the region of the typical [WC] PNNi. Obviously A 30 and A 78 are already well within the PG 1159 region.

Another observation indicating that the nature of the discussed objects is probably different from that of the [WC] PNNi can be made from observational appearances of the nebulae. The three objects which have already evolved to the PNN region after the late He-shell flash, i.e. A 30, A 58 and A 78, display H-defficient nebular regions inside the main nebula. As discussed above these regions have probably been formed during the flash when the central star was a born again AGB star. No such H-deficient regions have been detected inside any PN with the [WC] nucleus.

Thus the final conclusion of the discussion in this subsection is that the [WC] PNNi do not follow the evolutionary path of the PNNi for which we have direct observational evidences that they have experienced (or are experiencing) a late He-shell flash. Obviously the statistics is low and it would be premature to conclude that the late He-shell flash never gives origin to a [WC] PNN. Nevertheless the observational facts for the above five objects, at least, do not contradict this hypothesis.

6. Conclusions and discussion

We have made a thorough analysis of the available observational data for the PNe with H-deficient central stars. As we have shown in Sect. 3 an evolutionary sequence can be identified within this group of objects. The stars start their evolution as late-[WC], then become early-[WC] and end up as PG 1159 stars. This is however a general sequence and it can be that some individual objects evolve in a different way.

The analyses in Sects. 4 and 5 give arguments that the very late He-shell flash (born again AGB) is not the main evolutionary path giving origin to the H-deficient PNNi. We argue that the H-deficient central stars evolve directly from the AGB as do other PNNi in their majority. This conclusion is most evident for the [WC] PNNi and is consistent with the observed characteristics of the PG 1159 stars and their nebulae. Nevertheless it cannot be excluded that some H-deficient PNNi have been produced in the late He-shell flash. Indeed for some objects, i.e. A 30, A 58, A 78, FG Sge and V4334 Sgr, we have direct evidences that they have experienced a late He-shell flash. However, these objects are expected to evolve directly to the region of PG 1159 stars without passing through the [WC] region.

Our conclusion that the H-deficient PNNi mostly evolve directly from the AGB has serious implications. First, the mass loss from (at least some) stars leaving the AGB while burning helium in the shell has to remove all the mass of the H-rich envelope before the PN phase. This has not yet been predicted from any standard evolutionary modelling of the post-AGB phase. The point is that when the H-rich envelope drops below typically $10^{-3}\mathrm{M}_{\odot}$ the stellar effective temperature starts increasing, accordingly mass loss drops and is not able to remove the rest of the H-rich envelope before the onset of the PN phase. The analysis in Sect. 4 shows that the duration of the post-AGB (or proto-PN) phase is similar for the H-deficient PNNi as for the others. Thus a proto-[WC] PNN during a few thousand years gets rid of the entire H-rich envelope which implies a mass loss rate typically of $10^{-6}\mathrm{M}_{\odot}\ \mathrm{yr}^{-1}$. Similar mass loss rates are also observed in the [WC] phase. This can be interpreted as an indication that the yet unidentified mass loss mechanism responsible for the appearance (and evolution) of the [WC] PNNi resides beneath the H-rich envelope. One may speculate that He- and C-rich layers pushed up during the helium shell flash cool down and form a high opacity layer well below the stellar photosphere. Increased radiation pressure (due to high opacity and high luminosity during the flash) might lift up upper stellar layers and form an intense wind. A detailed radiation-hydrodynamic modelling of flashing AGB stars with small H-rich envelopes are obviously necessary.

The second implication results from the observed abundances in the [WC] PNNi. Spectroscopic analyses of the latest [WC] (i.e. youngest according to our analysis) stars show that from the very beginning of the [WC] phase the observed C abundance is comparable to that of He (e.g. Leuenhagen et al. 1996). This implies a very intense mixing in the He-rich layers during the He-shell flash. Standard treatment of convection gives models in which upper He-rich layers are composed of almost pure He (see e.g. discussion in Schönberner & Blöcker 1992). Significant overshooting seems to be required in order to account for the observed abundances (Herwig et al. 1997).

Acknowledgements. We thank the referee (D. Schönberner) for his remarks which have allowed us to improve our analysis and the text of the paper. This work was in part supported from grants No. 2.P03D.002.13 & 2.P03D.020.17 financed by the Polish State Committee for Scientific Research.

References

Abell G.O., 1966, ApJ 144, 259
Acker A., Köppen J., Stenholm B., Jasniewicz G., 1989, A&AS 89, 201
Acker A., Köppen J., Stenholm B., Raytchev B., 1991, A&AS 89, 237
Acker A., Ochsenbein F., Stenholm B., et al., 1992, Strasbourg-ESO Catalogue of Galactic Planetary Nebulae. ESO publication
Acker A., Górny S.K., Cuisinier F., 1996, A&A 305, 944
Acker A., Parthasarathy M., Stenholm B., 1999, Quantitative classification of [WC] nuclei of planetary nebulae. Preprint
Blöcker T., 1995, A&A 299, 755
Blöcker T., Schönberner D., 1997, A&A 324, 991
Bond H.E., Meakes M.G., Liebert J.W., Renzini A., 1993, In: Weinberger R., Acker A. (eds.) Proc. IAU Symp. 155, Planetary Nebulae. Kluwer, p. 499
Crowther P.A., De Marco O., Barlow M.J., 1998, MNRAS 296, 367
Cuisinier F., 1994, Ph.D. Thesis, Observatoire de Strasbourg
De Marco O., Barlow M.J., Storey P.J., 1997, MNRAS 292, 86
Dreizler S., Werner K., Heber U., 1995, In: Koester D., Werner K. (eds.) White Dwarfs. Springer, p. 160
Ford H.C., 1971, ApJ 170, 547
Górny S.K., 2000, Ap&SS in press
Górny S.K., Stasińska G., 1995, A&A 303, 893
Górny S.K, Tylenda R., Szczerba R., 1994, A&A 284, 949
Górny S.K., Stasińska G., Tylenda R., 1997a, A&A 318, 256

Górny S.K., Szczerba R., Zalfresso-Jundziłło M., 1997b, In: Habing H.J., Lamers H.J.G.L.M. (eds.) Proc. IAU Symp. 180, Planetary Nebulae. Kluwer, p. 229
Hamann W.-R., 1996, In: Jeffery C.S., Heber U. (eds.) Hydrogen-Deficient Stars. ASP Conference Series, p. 127
Hamann W.-R., 1997, In: Habing H.J., Lamers H.J.G.L.M. (eds.) Proc. IAU Symp. 180, Planetary Nebulae. Kluwer, p. 91
Hawley S.A., Miller J.S., 1978, ApJ 221, 851
Hazard C., Terlevich B., Morton D.C., Sargent W.L., Ferland G., 1980, Nat 285, 463
Heap S., 1982, In: De Loore C.W.H., Willis A.J. (eds.) Proc. IAU Symp. 99, Wolf-Rayet Stars: Observations, Physics, Evolution. Reidel, p. 423
Herwig F., Blöcker T., Schönberner D., El Eid M., 1997, A&A 324, L81
Iben I., 1984, ApJ 277, 333
Iben I., MacDonald J., 1995, In: Koester D., Werner K. (eds.) White Dwarfs. Springer, p. 48
Iben I., Renzini A., 1983, ARA&A 21, 271
Iben I., Kaler J.B., Truran J.W., Renzini A., 1983, ApJ 264, 605
Jacoby G.H., Ford H.C., 1983, ApJ 266, 298
Kerber, F., Köppen, J., Roth, M., Trager, S.C., 1999, A&A 344, L79
Kingsburgh R.L., Barlow M.J., 1994, MNRAS 271, 257
Koesterke L., Hamann W.-R., 1997, In: Habing H.J., Lamers H.J.G.L.M. (eds.) Proc. IAU Symp. 180, Planetary Nebulae. Kluwer, p. 114
Leuenhagen U., Hamann W.-R., Jeffery C.S., 1996, A&A 312, 167
Leuenhagen U., Koesterke L., Hamann W.-R., 1993, Acta Astron. 43, 329
Lundsröm, I., Stenholm, B. (eds.), 1996, In: Lundsröm, I., Stenholm, B. (eds.) Planetary Nebulas with Wolf-Rayet Type Nuclei. Ap&SS 238, No.1
Lutz J.H., 1978, In: Terzian Y. (ed.) Proc. IAU Symp. 76, Planetary Nebulae. Reidel, Dordrecht, p. 185
Méndez R.H., 1991, In: Michaud G., Tutukov A. (eds.) Proc. IAU Symp. 145, Evolution of Stars: The Photospheric Abundance Connection. Dordrecht, Kluwer, p. 375
Napiwotzki R., Schönberner D., 1995, A&A 301, 545
Napiwotzki R., Haas S., Schönberner D., 1996, In: Jeffery C.S., Heber U. (eds.) Hydrogen-Deficient Stars. ASP Conference Series, p. 213
Pollacco, D., 1999, MNRAS 304, 127
Philips J.P., 1998, A&A 340, 527
Reay N.K, Atherton P.D., Taylor K., 1983, MNRAS 203, 1079
Schönberner D., 1979, A&A 79, 108
Schönberner D., 1981, A&A 103, 119
Schönberner D., 1989, In: Torres-Peimbert S. (ed.) Proc. IAU Symp. 131, Planetary Nebulae. Kluwer, p. 463
Schönberner D., Blöcker T., 1992, In: Heber U., Jeffery C.S. (eds.) Atmospheres of Early Type Stars. Springer, p. 305
Seitter W.C., 1989, In: Torres-Peimbert S. (ed.) Proc. IAU Symp. 131, Planetary Nebulae. Kluwer, p. 315
Stanghellini L., Kaler J.B., 1989, ApJ 343, 811
Stasińska G., Tylenda R., Acker A., Stenholm B., 1992, A&A 266, 486
Stasińska G., Tylenda R., 1994, A&A 289, 225
Stasińska G., Górny S.K., Tylenda R., 1997, A&A 327, 736
Tylenda R., 1980, Acta Astron. 30, 433
Tylenda R., 1996, In: Jeffery C.S., Heber U. (eds.) Hydrogen-Deficient Stars. ASP Conference Series, p. 101
Tylenda R., Acker A., Stenholm B., 1993, A&AS 102, 595
Tylenda R., Górny S.K., 1993, Acta Astron. 43, 389
Tylenda R., Stasińska G., 1989, A&A 217, 209
Tylenda R., Stasińska G., Acker A., Stenholm B., 1994, A&AS 106, 559
Vassiliadis E., Wood P.R., 1994, ApJS 92, 125
Werner K., Dreizler S., Heber U., Rauch T., 1996, In: Jeffery C.S., Heber U. (eds.) Hydrogen-Deficient Stars. ASP Conference Series, p. 267
Werner K., Hamann W.-R., Heber U., et al., Wessolowski U., 1992, A&A 259, L69
Wood P.R., Faulkner D.J., 1986, ApJ 307, 659
Yudin B.F., Tatarnikov A.M., 1999, In: Le Bertre T., Lebre A., Waelkens C. (eds.) Proc IAU Symp. 191, Asymptotic Giant Branch Stars. ASP, p. 487